Inorganic Chemistry
Article

Inorg. Chem. **2009**, *48*, 6573–6583 **6573**
DOI: 10.1021/ic9004856

Gold Tetrahedra as Building Blocks in K_3Au_5Tr (Tr = In, Tl) and Rb_2Au_3Tl and in Other Compounds: A Broad Group of Electron-Poor Intermetallic Phases

Bin Li, Sung-Jin Kim, Gordon J. Miller, and John D. Corbett*

Ames Laboratory—DOE and Department of Chemistry, Iowa State University, Ames, Iowa 50011

Received March 11, 2009

The alkali-metal gold trielides K_3Au_5Tr (Tr = In (**I**), Tl (**II**)) and Rb_2Au_3Tl (**III**) have been obtained directly from the elements, and their orthorhombic structures determined by single-crystal X-ray diffraction means (**I/II**: *Imma*, a = 5.562(1), 5.595(1); b = 19.645(4),19.706(4); c = 8.502(2), 8.430(2) Å; Z = 4, respectively; **III**: *Pmma*, a = 5.660(1), b = 6.741(1), c = 9.045(2) Å, Z = 4). These exhibit zigzag chains of Tr that link puckered sheets (**I/II**) or chains (**III**) of gold tetrahedra condensed through shared vertices. The segregation of Au and Tr components is striking relative to the evidently stronger and preferred Au−Tr bonding in neighboring gold- and alkali-metal-poorer triel phases. The close packing of K/Rb (A) about the gold tetrahedra gives each A and Au_4 component 7−10 and 10 neighbors of the other type, respectively. Tight-binding−linear-muffin-tin-orbital−atomic sphere approximation band structure calculations show that the title phases lie near or at electronic pseudogaps. The gold substructure is the dominant feature of the densities of states, with moderately broad $5d^{10}$ features as favored by relativistic effects. Likewise, crystal orbital Hamilton population results indicate optimization of Au−Au bonding at the expense of the stronger heteroatomic Au−Tr interactions. Stabilization of these unusual structures appears to follow in part from the presence of numerous short and individually weak A−Au interactions, as manifested by appreciable mixing of s, p, and d valence orbitals on A into network bonding states, Au 5d in particular. These and related phases define a family of Au_4-based phases with particularly low e/a values of 1.2∼2.3 (over all atoms, omitting Au 5d), closely related to the cubic *Laves*-type structures. The same region also contains Tr-richer tunnel and network structures with relatively fewer cations that also appear to be dominated by Au−Au and Au−Tr bonding.

Introduction

The polyanionic chemistry of the triels (Tr) Ga, In, and Tl that is generated through their reduction by the more active metals turns out to be distributed over a remarkable variety of hitherto unprecedented species and structures, quite distinct from the behavior of Al. Our efforts have particularly pursued the chemistry of the heavier In and Tl, leading to the discovery of a considerable number of discrete triel clusters as well as networks among the relatively alkali-metal-rich binary systems.[1,2] Earlier attempts to substitute the electron-poorer Zn, Cd, Cu, Ag, and Ni into these cluster products in order to gain greater degrees of condensation, particularly for Ga,[3,4] were relatively unproductive. On the other hand, explorations of the alkali-metal-poorer A−Tr systems have led to numerous anionic network structures, as in KNa_3In_9,[5] $K_{39}In_{80}$,[6] and $K_{34}In_{105-x}Li_x$.[7]

By far, the most productive third element in these explorations has been gold. This expansion started with the novel ternary alkaline-earth-metal (Ae) examples Ba_2AuIn_7,[8] $BaAuTr_3$ (Tr = In, Tl),[9] and $BaAu_{0.4}In_{1.6}$,[10] in which the Ae's are characteristically well encapsulated within the Au−Tr networks. Surprisingly, five distinctive tunnel structures exist in A−Au−In systems, A = K, Rb.[11,12] The considerable variety among these polar intermetallic phases appears to depend subtly on stoichiometry, lower e/a values (valence electrons per atom, omitting Au $5d^{10}$) in the polyanions, tight cation−anion packing, and, especially, the dominance of evidently strong Au−In bonding. Gold appears to play a substantial role in these because of relativistic effects[13] that serve to decrease its effective size; increase its 5d and 6s orbital bonding; and therewith enhance its electronegativity, overlap

*To whom correspondence should be addressed: E-mail: jcorbett@iastate.edu.

(1) Corbett, J. D. In *Chemistry, Structure and Bonding of Zintl Phases and Ions*; Kauzlarich, S., Ed.; VCH Publishers: New York, 1996, Chapter 3.
(2) Corbett, J. D. *Angew. Chem., Int. Ed.* **2000**, *39*, 670.
(3) Henning, R. W. Ph.D. Dissertation, Iowa State University, Ames, IA, **1998**.
(4) Henning, R. W.; Corbett, J. D. *J. Alloys Compd.* **2002**, *338*, 4.
(5) Li, B.; Corbett, J. D. *Inorg. Chem.* **2002**, *41*, 3944.
(6) Li, B.; Corbett, J. D. *Inorg. Chem.* **2003**, *42*, 8768.
(7) Li, B.; Corbett, J. D. *J. Am. Chem. Soc.* **2005**, *127*, 926.
(8) Liu, S.; Corbett, J. D. *Inorg. Chem.* **2004**, *43*, 2471.
(9) Liu, S.; Corbett, J. D. *Inorg. Chem.* **2004**, *43*, 4988.
(10) Dai, J.-C.; Corbett, J. D. *Inorg. Chem.* **2006**, *45*, 2104.
(11) Li, B.; Corbett, J. D. *J. Am. Chem. Soc.* **2006**, *128*, 12392.
(12) Li, B.; Corbett, J. D. *Inorg. Chem.* **2007**, *46*, 6022.
(13) (a) Pyykkö, P. *Chem. Rev.* **1988**, *88*, 63. (b) Pyykkö, P. *Angew. Chem., Int. Ed.* **2002**, *41*, 3573.

© 2009 American Chemical Society
Published on Web 06/16/2009

(bond) populations, and, equivalently, heteroatomic bond energies with p metals.

The present investigations concern the extensions of this chemistry to remarkable gold-richer (and relatively cation-richer) phases in which Au_4 tetrahedra share vertices to generate polygold chains in Rb_2Au_3Tl (**III**) or puckered sheets in K_3Au_5Tr (Tr = In (**I**), Tl (**II**)). The second structure type has already been reported for the neighboring K_3Au_5-Pb, along with the note of its relationship to $NaAu_2$[14] in projection but without comment on the bonding.[15] In considerable contrast, the triel atoms now serve to link these gold arrays via zigzag chains of four-bonded (4b) In or Tl rather than to form the heteroatomic Au−Tr bonded networks commonly found in gold-poorer compounds (above). Less condensed but still tetrel-linked versions were also reported as early as 1981 for $A_4Au_7Tt_2$ phases (A = K−Cs; Tt = Ge, Sn), in which tetrahedral gold dimers $Au(Au_3)_2$ are interconnected by Tt_2 units.[16−18] Other less regular and less tractable polygold structures will be noted later. At the other extreme, many members of this family of compounds can be seen to derive from $NaAu_2$[14] (*Friauf*−*Laves* phase of $MgCu_2$ type[19]), which is built of gold tetrahedra sharing all vertices, with Mg replaced by sodium. A general theme among these unusual Au_4-based structures is that they possess particularly low electron counts per network atom (< 2), within which the cations at first glance seem to serve mainly as spacers and electron donors, as is common in many related polar intermetallic compounds as well as in *Zintl* phases.

Experimental Section

Synthesis. All reactants and products were handled in a dry N_2 atmosphere (H_2O level < 0.1 ppm) in a glovebox. The procedures followed general methods employed previously.[11,12] Reactions were allowed to take place with between ∼300 and 400 mg of the high purity elements: K and Rb, 99.9% (Alfa-Aesar); Au, 99.997% (Ames Lab); In, 99.99% (Alfa-Aesar); Tl, 99.998% (Johnson-Matthey). These were carried out in tube furnaces with the mixed metals sealed within 6−9-mm-diameter Ta containers that were, in turn, enclosed in evacuated and well-baked silica jackets to protect the former from air. The reactions generally followed the sequence of heating at 650 °C for 12 h, cooling at 5°/h to 450 °C, equilibrating there for 160 h, and slow cooling to room temperature. K_3Au_5Tl (**II**) and Rb_2Au_3Tl (**III**) were discovered during attempts to synthesize AAu_4Tl_2 analogues of AAu_4In_2 and other tunnel structures.[11,12] Later reactions starting with compositions of the refined structures all gave high yields of the products (>95 vol % on the basis of observed versus calculated powder pattern data). The K_3Au_5In (**I**) result followed directly, whereas attempts to prepare the K or In analogues of Rb_2Au_3Tl were unsuccessful. The compounds are silver gray in color and sensitive to air.

X-Ray Diffraction Studies. Powder diffraction data were collected with the aid of a Huber 670 Guinier powder camera equipped with an area detector and Cu Kα radiation (λ = 1.540598 Å). The samples were homogeneously dispersed in a glovebox between two Mylar sheets with the aid of a little vacuum grease. These were in turn held between split Al rings that provided airtight seals. Unit cell parameters were refined using the WinXPow program[20] and subsequently applied to distance calculations after single-crystal structure refinements.

Single-crystal diffraction data sets were collected at 293(2) K with the aid of Mo Kα radiation and, for the isostructural **I**/**II**, a Bruker SMART APEX CCD diffractometer. The data came from three sets of 606 frames with 0.3° scans in ω and exposure times of 10 s per frame. The reflection intensities for each were integrated with the SAINT subprogram in the SMART software package.[21] The space group determination was done with the aid of XPREP and the SHELXTL 6.1 software package. Empirical absorption corrections for both were first made with the aid of the SADABS program.[22] The structures were solved by direct methods with the aid of SHELXTL 6.1 and subsequently refined in the indicated centrosymmetric space group *Imma* by full-matrix least-squares on F_o^2, ultimately with anisotropic thermal parameters and a secondary extinction parameter. However, the semiempirical absorption corrections (SADABS) were evidently inadequate for **II**, as the refined U_{ii} magnitudes were very extreme for the three independent Au atoms (e.g., ∼0.01:0.01−5:5−13 Å^2). Therefore, numerical absorption corrections using X-Red and X-SHAPE in the X-Area package[23] were applied with good results. With forethought, the single-crystal diffraction data for **III** were collected on a STOE IPDS 2 diffractometer and handled with the accompanying package programs, including the numerical absorption corrections, again with good results. Both the high proportions of sixth period elements in the two Tl compounds and the crystal sizes employed were presumably responsible for the empirical absorption correction problems. Some data collection and refinement parameters are collected in Table 1. The atom positional data for the three structures are given in Table 2, and important bond distances are listed in Table 3. The three CIF outputs and a summary of parameters are provided in the Supporting Information.

Electronic Structure Calculations. Tight-binding electronic structure calculations were performed for all three phases according to the linear muffin-tin-orbital (LMTO) method in the atomic sphere approximation.[24] The radii of the Wigner−Seitz (WS) spheres were assigned automatically so that the overlapping potentials would be the best possible approximations to the full potentials.[25] The calculations used a basis set of K-4s/(4p)/3d, Rb-5s/(5p)/4d/(4f), Au-6s/6p/5d/(5f), In-5s/5p/(4d)/(4f), and Tl-6s/6p/(5d)/(5f) (downfolded[26] orbitals in parentheses), and the reciprocal space integrations were performed on grids with 621 (**I**/**II**) and 405 (**III**) irreducible *k* points. Scalar relativistic corrections were included. For space filling within the atomic sphere approximation, empty spheres (ES) were also introduced where needed. All sphere positions and radii were calculated automatically within the limit of 18% overlap between any atom-centered spheres; the WS radii [Å] were K, 1.94−2.02; Au, 1.52−1.66; In, 1.58; Tl, 1.61−1.62; ES, 0.58−0.89. Calculations on the centered **I** and **II** were performed for the primitive cell with two formula units per cell.

For bonding analysis, the energy contributions of all electronic states for selected atom pairs were calculated as a function of the energy according to the crystal orbital Hamilton population (COHP) method.[27] Integration over all filled states gives ICOHP values as measures of relative bond strengths (overlap populations). The Fermi levels were all set to zero, and the COHP data are necessarily plotted with reversed values

(14) Haucke, W. *Naturwiss*. **1937**, *25*, 61.
(15) Zachwieja, U.; Wlodarski, J. *Z. Anorg. Allg. Chem*. **1998**, *624*, 1569.
(16) Sinnen, H.-D.; Schuster, H.-U. *Z. Naturforsch*. **1981**, *36b*, 833.
(17) Zachwieja, U. *Z. Anorg. Allg. Chem*. **1998**, *621*, 975.
(18) Zachwieja, U.; Wlodarski, J. *Z. Anorg. Allg. Chem*. **1998**, *624*, 1443.
(19) (a) Friauf, J. B. *J. Am. Chem. Soc*. **1927**, *49*, 3107. (b) Friauf, J. B. *Phys. Rev*. **1927**, *29*, 34.
(20) *WinXPow 2.10*; Stoe & Cie GmbH: Darmstadt, Germany, 2004.
(21) *SMART*; Bruker AXS, Inc.; Madison, WI, 1996.
(22) Blessing, R. H. *Acta Crystallogr*. **1995**, *A51*, 33.
(23) (a) *X-Red*, version 1.22; Stoe & Cie GmbH: Darmstadt, Germany, 2001. (b) *X-Shape*, version 1.06; Stoe & Cie GmbH: Darmstadt, Germany, 1999.
(24) Krier, G.; Jepsen, O.; Burkhardt, A.; Andersen, O. K. *TB-LMTO-ASA Program*, version 4.7; Max-Planck-Institut für Festkörperforschung: Stuttgart, Germany, 1995.
(25) Jepsen, O.; Andersen, O. K. *Z. Phys. B* **1995**, *97*, 35.
(26) (a) Lambrecht, W. R. L.; Andersen, O. K. *Phys. Rev. B* **1986**, *34*, 2439. (b) Löwdin, P. *J. Chem. Phys*. **1951**, *19*, 1396.
(27) Dronskowski, R.; Blöchl, P. E. *J. Phys. Chem*. **1993**, *97*, 8617.

Table 1. Some Crystal and Refinement Data for K_3Au_5In (**I**), K_3Au_5Tl (**II**), and Rb_2Au_3Tl (**III**)

compounds	**I**	**II**	**III**
fw	1216.9	1306.5	966.2
space group, Z	*Imma* (No. 74), 4	*Imma* (No. 74), 4	*Pmma* (No. 51), 2
unit cell params[a]			
a/Å	5.562(1)	5.595(1)	5.660(1)
b/Å	19.645(4)	19.706(4)	6.741(1)
c/Å	8.502(2)	8.430(2)	9.045(2)
V/Å^3	928.9(3)	929.5(3)	345.1(1)
d_{calcd}/g cm^{-3}	8.70	9.34	9.30
μ/mm^{-1} (Mo Kα)	82.36	97.15	100.73
data/restraints/params	634/0/31	636/0/31	549/0/24
R_1/wR_2 [$I > 2\sigma(I)$]	0.027/0.061	0.043/0.106	0.046/0.105
R_1/wR_2 (all data)	0.030/0.062	0.046/0.107	0.062/0.110
largest diff. peak, hole/e Å^{-3}	+2.94 [0.85 Å from Au1], −3.30 [0.66 Å from Au2]	+4.44 [0.89 Å from Au3], −2.77 [1.44 Å from Tl]	+5.43 [0.79 Å from Au2], −3.74 [1.42 Å from Au2]

[a] Data refined from Guinier powder patterns.

Table 2. Atomic Coordinates and Equivalent Isotropic and Anisotropic Displacement Parameters (Å$^2 \times 10^3$) for K_3Au_5In (**I**), K_3Au_5Tl (**II**) (second lines), and Rb_2Au_3Tl (**III**)[a]

atom	Wyck.	x	y	z	U_{eq}	U_{11}	U_{22}	U_{33}
			K_3Au_5Tr (Tr = In (**I**), Tl (**II**))					
Au1	8*h*	0	0.1452(1)	0.0349(1)	10(1)	11(1)	7(1)	12(1)
		0	0.1438(1)	0.0415(1)	21(1)	16(1)	17(1)	30(1)
Au2	8*g*	1/4	0.0655(1)	1/4	12(1)	8(1)	15(1)	12(1)
		1/4	0.0618(1)	1/4	18(1)	10(1)	22(1)	23(1)
Au3	4*a*	0	0	0	9(1)	12(1)	6(1)	8(1)
		0	0	0	17(1)	12(1)	16(1)	21(1)
Tr	4*e*	0	1/4	0.8353(2)	11(1)	16(1)	6(1)	10(1)
		0	1/4	0.8364(2)	22(1)	22(1)	17(1)	26(1)
K1	8*h*	0	0.0879(2)	0.6253(5)	16(1)	13(2)	18(2)	17(3)
		0	0.0879(3)	0.6223(8)	25(1)	16(3)	28(2)	29(3)
K2	4*e*	0	1/4	0.3777(7)	22(1)	15(3)	28(3)	21(3)
		0	1/4	0.380(1)	31(2)	21(4)	41(5)	31(5)
			Rb_2Au_3Tl (**III**)					
Tl	2*f*	1/4	1/2	0.5744(2)	22(1)	28(1)	19(1)	20(1)
Au1	4*k*	1/4	0.2095(2)	0.7848(1)	22(1)	22(1)	20(1)	23(1)
Au2	2*a*	0	0	0	19(1)	18(1)	21(1)	18(1)
Rb1	2*e*	1/4	0	0.3741(5)	29(1)	24(2)	35(2)	28(2)
Rb2	2*f*	1/4	1/2	0.1328(5)	27(1)	23(2)	28(2)	30(2)

[a] $U_{12} = U_{13} = U_{23} = 0$.

with respect to energy (i.e., −COHP vs E), as negative values correspond to bonding interactions.

Semiempirical extended-Hückel (EHTB) band calculations[28] allow Mulliken population analyses at each atomic site relative to average e/a (or vec) values, Au contributing one electron in these cases. Such results provide some helpful guidance as to the intrinsic site charge differences and atom-type segregations (coloring) within a particular structural framework.[29] In order to avoid bias arising from the diverse atom types, the relative site populations were calculated for **II** and **III** with the same atomic parameters (Tl here) on all Au and Tl sites. Mulliken populations for valence orbital occupations were evaluated by integration over a set of 216 k points in the irreducible wedge of the Brillouin zone. Atomic orbital energies and exponents employed in the calculations for Tl were (H_{ii} = orbital energy, eV; ξ = Slater exponent, respectively): Tl = 6s: −11.60, 2.37; 6p: −5.80, 1.60.[30]

Results and Discussion

Structures of K_3Au_5In and K_3Au_5Tl. Figure 1 shows two views of the K_3Au_5In (**I**) structure, a result that is also shared by its thallium analogue (Tables 1−3). The structure itself is the same as that reported for K_3Au_5Pb in 1998.[15] Zigzag chains of gold tetrahedra that share three of four vertices with each other generate puckered sheets of gold tetrahedra around the $a-c$ plane, Figure 1a. The lattice is shown along c in Figure 1b, and the connectivity is made clearer by the more local [010] view of the chain construction in Figure 2a: All gold tetrahedra share 6b−Au2 and 6b−Au3 vertices, each of the remaining 4b−Au1 atoms being connected to one Tr atom (blue). The Tr atoms in turn lie in parallel zigzag chains with homoatomic distances of 3.136(2) Å and 3.157(1) Å in **I** and **II**, respectively, values that are comparable to those in NaIn, 3.16 Å, and NaTl, 3.24 Å.[31] The continuation of the former motif in the plane of Figure 2a via Au3 generates the puckered sheets seen end-on in Figure 1a. Figure 2b illustrates an important feature: the notably uniform and compact arrangement of potassium cations around each tetrahedron, 10 of these collectively bridging all edges and capping all faces of the cluster. (Three other gold tetrahedra and one indium atom are bonded at the vertices.) As illustrated in the Supporting Information (Figure S1), each of the two types of K is tightly associated with the gold chains. The K1 atoms appear well-bound to the gold chain, with 10 neighbors at 3.29−3.66 Å, nine of these capping three triangular faces on the condensed Au_4 units (a small red dot marks a K1 position in Figure 2a.) Half as many K2 atoms lie near the centers of the larger channels through the structure (Figure 1a), between the planes of In atoms and two Au chains (Figure 1b), with six Au neighbors at 3.54−3.57 Å. Average distances are d(K1−Au) = 3.47 Å and d(K2−Au) = 3.54 Å, and K2 has three additional contacts with In while K1 only has one (d(K1−In) = 3.65 Å; av. d(K2−In) = 3.76 Å). These observations are consistent with a significant feature of the structure,

(28) Ren, J.; Liang, W.; Whangbo, M.-H. *CAESAR for Windows*; Prime-Color Software, Inc., North Carolina State University: Raleigh, NC, 1998.

(29) (a) Lee, C.-S.; Miller, G. J. *J. Am. Chem. Soc.* **2000**, *122*, 4937. (b) Lee, C.-S.; Miller, G. J. *Inorg. Chem.* **2001**, *40*, 338. (c) Li, B.; Corbett, J. D. *Inorg. Chem.* **2004**, *43*, 3582. (d) Nordell, K. J.; Miller, G. J. *Angew. Chem., Int. Ed. Engl.* **1997**, *36*, 2008.

(30) (a) Kang, D. B.; Jung, D.; Whangbo, M.-H. *Inorg. Chem.* **1990**, *29*, 257. (b) Janiak, C.; Hoffmann, R. *J. Am. Chem. Soc.* **1990**, *112*, 5924.

(31) (a) Zintl, E.; Neumayr, S. *Z. Phys. Chem.* **1933**, *B20*, 272. (b) Zintl, E.; Dullenkopf, W. *Z. Phys. Chem.* **1932**, *B16*, 195.

Table 3. Selected Interatomic Distances [Å] in K_3Au_5In, K_3Au_5Tl, K_3Au_5Pb, and Rb_2Au_3Tl

atom pair	K_3Au_5In	K_3Au_5Tl	K_3Au_5Pb[a]	Atom pair	Rb_2Au_3Tl
Au1−M[b]	2.668(1)	2.715(1)	2.694(1)	Au1−Tl × 2	2.730(2)
Au1−Au2 × 2	2.780(1)	2.767(1)	2.737(1)	Au1−Au2 × 2	2.790(1)
Au1−Au3	2.868(1)	2.856(1)	2.817(1)	Au1−Au1[c]	2.825(2)
Au2−Au2 × 2	2.781(1)	2.798(1)	2.823(1)	Au2−Au2 × 2[c]	2.830(1)
Au2−Au3 × 2	2.848(1)	2.808(1)	2.836(1)		
M−M[b] × 2	3.136(2)	3.154(2)	3.157(1)	Tl−Tl	3.134(1)

[a] Reference 15. [b] M = In, Tl or Pb. [c] Not comparable to this distance in K_3Au_5Tr.

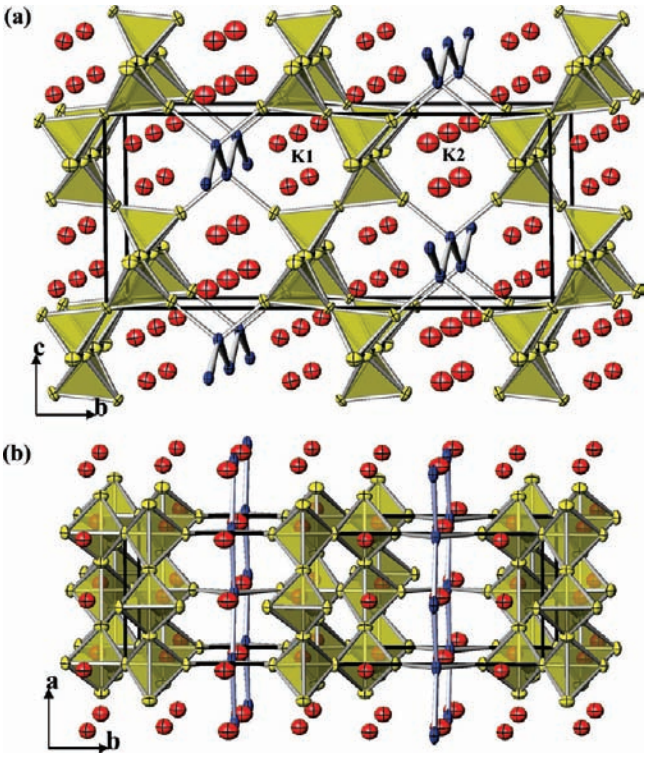

Figure 1. General views of K_3Au_5Tr as (a)∼[100] and (b)∼[001] sections. The triel, Au, and alkali metal atoms are blue, yellow, and red, respectively, throughout (97% probability ellipsoids).

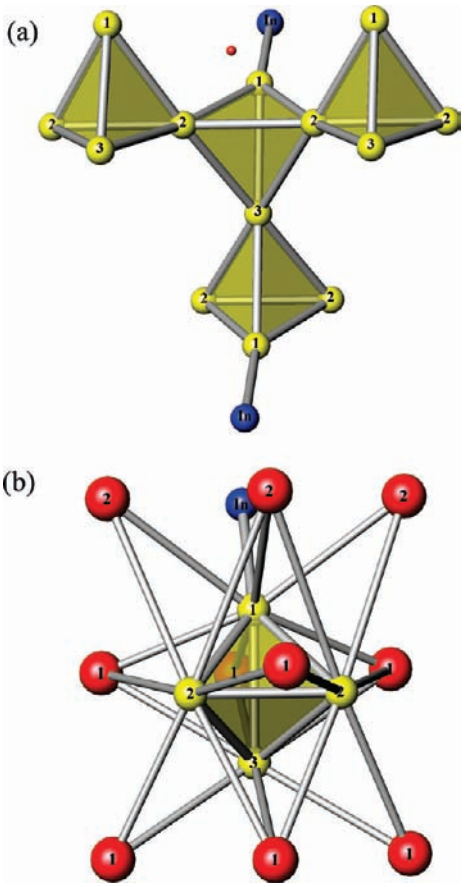

Figure 2. Structural details for K_3Au_5Tr. (a) Cluster condensation mode in which each Au_4 tetrahedron shares three vertexes with other like tetrahedra, with the Au1 vertex *exo*-bonded to a Tr atom. This motif generates infinite puckered sheets about the (020) planes. (b) All 10 edges and faces of the Au_4 tetrahedron are bridged or capped by K atoms.

a tight binding of K to the electronegative Au. The isostructural thallium phase (**II**) is closely related, as will be seen later in distance comparisons for these and a previously reported isotype with the neighboring lead, K_3Au_5Pb.[15] Such tight geometric "solvation" of anions by cations, and vice versa, is quite general among a wide variety of such intermetallic "salts". This characteristic is responsible for the general ability to tune A−A′−In and other systems to generate alternate (and often more complex) structures through the use of mixed cations of different sizes or charges in the syntheses.[2] This process is highly exploratory, too.

Structure of Rb_2Au_3Tl. This new structure type, Figure 3, appeared when cation substitution was attempted in **II**. (Note that axial directions have been switched relative to Figure 1a in order to show that the chains have similar features. The principal symmetry change is the loss of the body-centering operation.) The structure shows a similar bonding theme to that in **I**/**II**, that is, vertex-sharing of gold tetrahedra, but the degree of Au_4 condensation is reduced to chains following its smaller proportion. The simple condensation mode at 6b−Au2 that produces alternation of the Au_4 orientations along ∼[001] is clearer in Figure 4a, this leaving two Au1 atoms only four-bonded, once to a Tl atom in zigzag chains (d(Tl−Tl) = 3.134(1) Å) that again bridge four columns of gold tetrahedra. The quite specific environment about each Au_4 remains (Figure 4b vs Figure 2b), although this tetrahedron is less distorted than before because of the simpler chain structure.

The cations can be differentiated by their characteristics along the *b* direction, Figure 3a; Rb1 and Rb2 atoms lie around the two horizontal planes that center the In and the Au chains, respectively. Each Rb1 atom caps side faces of alternate Au_4 groups in the *c* direction, and each also bridges a backside Au1−Au1 edge in the opposed chain (3.97 Å). The Rb2 atoms lie near the horizontal planes of the gold cluster and have 10 Au neighbors mainly along *b*, bridging five pairs of Au1−Au2 edges

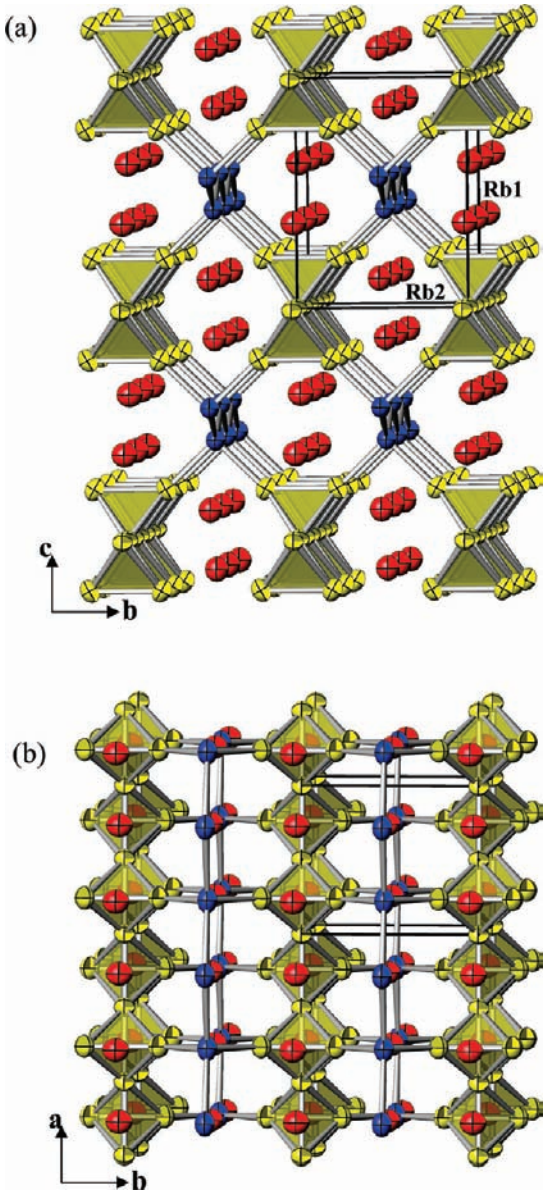

Figure 3. General views of Rb_2Au_3Tl in (a) ~[100] and (b) ~[001] sections.

in two separate chains. Again, the average distances (d(Rb1−Au) = 3.65; d(Rb2−Au) = 3.69; d(Rb1−Tl) = 3.83; d(Rb2−Tl) = 3.91 Å) show a closer bonding of Rb to Au. Figure S1 illustrates all of the cation environments, see the Supporting Information.

From a topologic point of view, both title structures can be regarded as Tr-substituted $(AB_2)_n$ compounds that are structurally derived from the cubic *Friauf*−*Laves* phase $NaAu_2$,[15] in which gold tetrahedra share all vertices. The Na atoms cap faces on four tetrahedra or, equivalently, center truncated gold tetrahedra (see Figure S5, Supporting Information). As sketched in Figure 5, both structures can be generated from $NaAu_2$ (left) by partial replacement of a certain one-third (**I**/**II**) or one-half (**III**) of the Au tetrahedra (black) with Tr atoms (blue). The substitutions lie in rows along horizontal directions and order along the projection axes such that strings of Au tetrahedra are converted into zigzag chains of Tr along that axis. (The altered product stoichiometries arise as marked

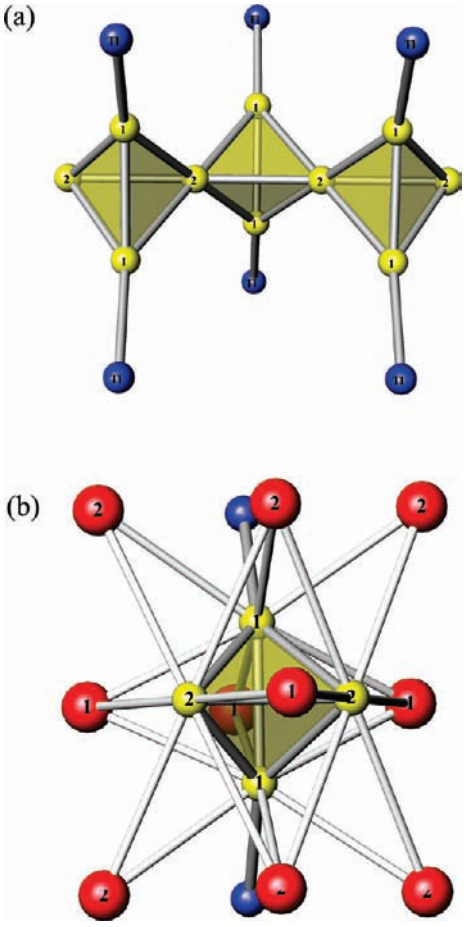

Figure 4. Structural details for Rb_2Au_3Tl. (a) The condensation mode in which each Au_4 tetrahedron shares two vertexes with like tetrahedra and the other two vertexes are *exo*-bonded to Tl. (b) All 10 edges and faces of the Au_4 tetrahedron are again bridged or capped by Rb atoms.

because each tetrahedron in $NaAu_2$ contains a net of two Au atoms.)

Distance variations among the three isotypic K_3Au_5M phases (M = In, Tl, Pb) are rather small, Table 3. The most regular trend is a shortening of the Au1−Au2 and Au1−Au3 distances around the Au1 vertices bonded to M from In to Tl to Pb (by up to 0.05 Å). This might arise if the Au−M bonds were to weaken in this order. A more remote comparison between the two Tl structures shows only small increases (up to 0.03 Å) in Au−Tl and Au−Au distances between the 3−5−1 and the 2−3−1 compositions. However, there are some clearer contrasts in relative Au−Au−Au angles between the two structure types. In both cases, those around the tetrahedra are around 60° (or multiples thereof), except in the tetrahedra bridged by six-bonded Au2 atoms along a in **I** and **II**, for which deviations of 6−12° are found. These presumably reflect some strain, as can be imagined to originate because the tetrahedra tilt in alternate directions along the linear Au2 string, Figure 1a. The Au−Au distances in these also pair off, those around 6b−Au2 being 2.77−2.80 Å for the most part, and a little larger around 6b−Au3, 2.81−2.87 Å. This may arise from distinct bond population differences (below). These distances map onto those in the simpler Rb_2Au_3Tl structure rather well, generally with small increases. The above group of smaller d(Au−Au)'s in K_3Au_5Tr are, in

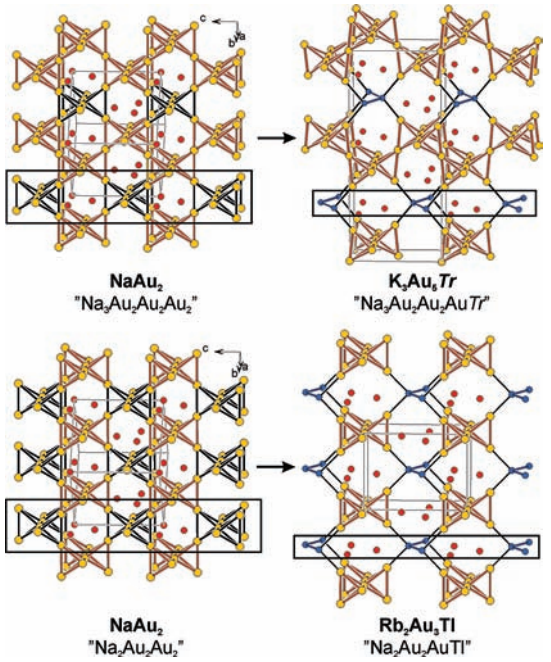

Figure 5. The structures of the title phases ([100] views, right) can be derived from the cubic *Laves*-type $NaAu_2$ (left, [110] view) by replacement of one-third (**I**/**II**) and one-half (**III**) of the Au tetrahedra (black) with Tr atoms (blue). The substitution positions lie in layers along the indicated *c* directions and repeat in chains along the projection axes. Cations remain in the same general positions.

general, comparable to the smallest in the similarly gold-rich $Ca_4Au_{10}In_3$,[32] $SrAu_4In_4$,[33] and $Cs_4Au_7Sn_2$,[18] but they are still greater than those in the irregular K_4Au_8Ga[34] (2.69 Å) and around the unusual square-planar Au atoms that lie between chains of tetrahedra in Rb_3Au_7 (2.63 Å)[35] (these two unusual phases are tabulated later).

Differences in Bond Types Around Au. These new structures afford a different version of mixed polyatomic anion chemistry in ternary polar intermetallics. They are not only the most gold-rich examples, but the unusual partial segregation of the Au from Tr and its clustering into chains are also very striking. (They are rivaled in this respect, however, by some forthcoming Au−Sn examples.[36]) In contrast, many other relatively cation-poorer A−Au−M (M = In, Sn) compounds feature more-or-less alternating atoms in the intermetallic polyanions and therefore a majority of short Au−In or Au−Sn bonds instead: KAu_4Sn_6, KAu_3Sn_3, and so forth;[37] $SrAu_{\sim4}In_{\sim4}$; and $Sr_4Au_9In_{13}$,[33] for instance. This characteristic is thought to reflect the substantial differences in the heteroatomic Mulliken electronegativities (In, 3.1; Tl, 3.2; Sn, 4.3 versus Au, 5.8 eV[38]) and, accordingly, significantly greater heteroatomic bond overlap populations (∼bond strengths). These distinctions may also be reinforced by the smaller numbers of cations sequestered in these networks as well as the higher charges on some. In contrast, the present compounds, with higher proportions of both gold in the networks and cations per network atom, exhibit an unusual converse disposition: separate zigzag chains of four-bonded In or Tl atoms that have equal numbers of Au−Tr and Tr−Tr bonds.

Interactions of the network atoms with the cations are also well-differentiated in the present phases, perhaps in part because both the extreme gold contents and the rather open networks favor (or allow) 7 to 10 Au contacts with each cation, from ∼3.30 Å (K) or 3.47 Å (Rb) up to about 4.0 Å. The cation neighbors are quite uniformly distributed among the gold atoms. In contrast, there are only two or three *d*(A−Tr) at ≥3.65 Å in the first coordination sphere (Figure S1, Supporting Information). The well-localized cations, and the alternating lateral Au_4 and In_2 bands that define the tunnel walls in KAu_4In_2, yield extremes of 3.38 Å (×8) and 3.92 Å (×4) for K−Au and K−In separations,[11] and other tunnel structures are similar in the shortest of each bond type.[12] (However, −ICOHP values per bond for K−Au and K−In in these last are less than 1% of those for each Au−Au and Au−In contact, in contrast to the present results, below). Comparable distinctions are also found within the more flexible networks in the 3D structures of $SrAu_{\sim4}In_{\sim4}$ and $Sr_4Au_9In_{13}$, each with 6-fold Sr−Au interactions down to ∼3.35 Å,[33] but not in KAu_4Sn_6 and KAu_3Sn_3.[37] The substantial electronegativity differences between active-metal cations and gold are presumably important in these situations and, probably, the smaller proportion of cations as well. But there may be complex geometric factors present, too. One remarkable and contrary example concerns the Ca atoms in the 1/1 quasicrystal approximant $Ca_3Au_{12.2}In_{6.3}$ ($Im\bar{3}$), which define an icosahedron that is bound between two concentric gold-rich Au/In shells as a part of a particularly compact, multiply endohedral cluster array. Here, Ca has 16 Au/In neighbors, all at substantially the same short distance, ∼3.25 Å.[39]

Distribution of Atom Types. A useful concept is that the atom distributions in many structures are intrinsic when viewed in terms of atom site populations or charge distributions. In other words, the more complex structures generally "know" which atom types belong on which sites, and there are substantially no coloring uncertainties.[29] The relative Mulliken site populations can be readily estimated from EHTB calculations if the same atom type is distributed over all of the refined positions, so as to avoid introduction of any bias from atom parameter differences. Figure 6 shows the relative populations of the different position types (that is, the calculated populations at each less the vec (valence electron concentration) as a function of vec for the network atoms in (a) K_3Au_5Tl and (b) Rb_2Au_3Tl, as deduced with thallium parameters on all Au and Tl sites. (The same relative results are obtained with an all-gold model.) The more electronegative gold atoms lie on the electron-richer sites (black, green, and red for Au1, Au2, and Au3 positions, respectively), with a bridging Tr intermediate (blue). Heteroatomic doping of these phases so as to alter the total valence electron counts would not seem to affect distributions greatly, although we have no a priori knowledge about a most important factor, *alternative* products and their structures.

(32) Lin, Q.; Corbett, J. D. *Inorg. Chem.* **2007**, *46*, 8722.
(33) Palasyuk, A.; Dai, J.-C.; Corbett, J. D. *Inorg. Chem.* **2008**, *47*, 3128.
(34) Zachwieja, U.; Wlodarski, J. *Z. Anorg. Allg. Chem.* **2000**, *626*, 1867.
(35) Zachwieja, U. *J. Alloys Compd.* **1993**, *199*, 115.
(36) Li, B.; Kim, S.-J.; Miller, G. J.; Corbett, J. D. In preparation.
(37) Li, B.; Corbett, J. D. *Inorg. Chem.* **2008**, *47*, 3610.
(39) Lin, Q.; Corbett, J. D. *J. Am. Chem. Soc.* **2007**, *129*, 6789.

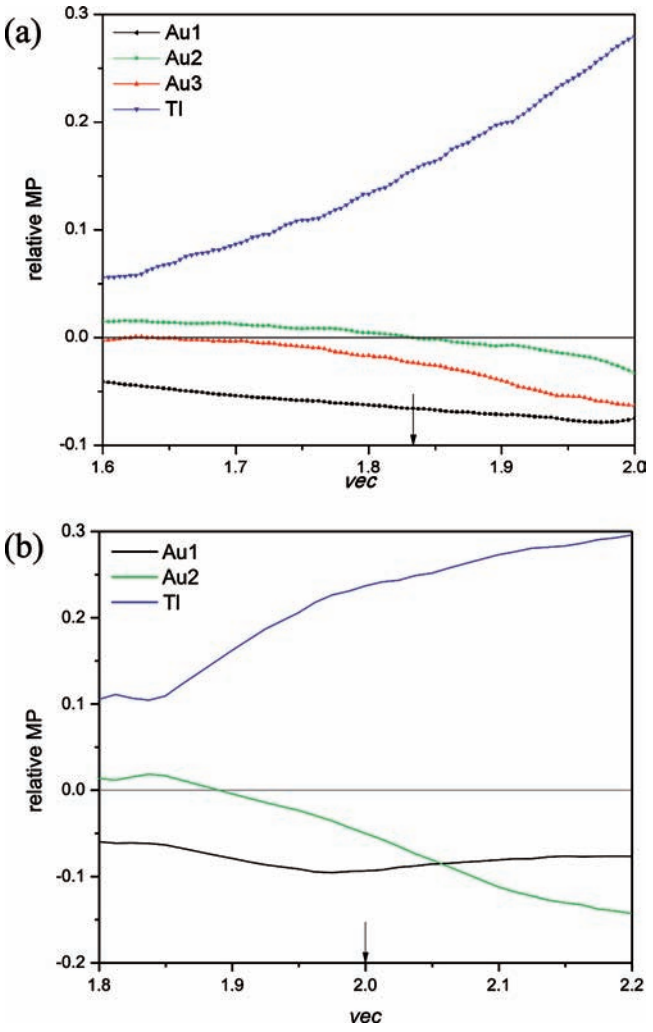

Figure 6. (a) The vec (valence electron concentration) versus relative Mulliken populations calculated by the EHTB method on the basis of a Tl_5Tl model and K_3Au_5Tl crystallographic data. Indicated with an arrow is the vec = (3 + 5 + 3)/6 for $\{Au_5Tl\}^{3-}$. (b) The vec versus relative Mulliken populations calculated on the basis of the $TlTl_3Tl$ model and Rb_2Au_3Tl crystallographic data. Indicated with an arrow is the vec = (2 + 3 + 3)/4 for $\{Au_3Tl\}^{2-}$.

Electronic Structures. The total densities-of-states (DOS) and individual atom projections for K_3Au_5Tl (**I**), K_3Au_5In (**II**), and Rb_2Au_3Tl (**III**) are shown as a function of energy in Figure 7a. The corresponding −COHP results for each atom pair type are in Figure 7b for the totals per cell and in Figure 7c for the average bonds. The last provides a clearer view of relative bond values without the distortion caused by wide variations in the relative number of bonds of each type in the structures. Partial DOS projections for each orbital and atom type are included in the Supporting Information.

The DOS generally feature broad dispersive valence bands through which the Fermi levels cut at moderately large values in **I/II** and at a local minimum for **III**. However, moderate pseudogaps also lie at only about 0.75 s and p electrons per formula unit above E_F (red dashed lines) in **I/II**, just above a total of 61 e^- at E_F. The narrow interval contains further bonding Au−Tr and Tr−Tr and nearly nonbonding Au−Au states. Therefore, modest electron doping should be possible, but the advantages may be small—the existence of the one-electron-richer K_3Au_5Pb[15] already points in this direction. The valence bands for all three cases are dominated by Au contributions followed by significantly smaller and approximately equal amounts from the A and Tr. Fat-band diagrams (Figure S2, Supporting Information) show that the Au valence orbitals in **I/II** are rather dispersed, reflecting the clustering, and band crossings suggest the phase to be a 3D metallic conductor. The contrary band structure of **III** shows only a few band crossings, and the dispersion is less pronounced. In all three cases, scalar relativistic effects lead to a destabilization of the 5d orbitals by ∼+2 eV with respect to the 6s states, which appear at slightly lower energies (−0.5 eV). Moderate splittings (∼2 eV) of the gold 5d DOS are found for the 6b−Au atoms (Figure S3, Supporting Information). On the other hand, the more exposed and less saturated 4b−Au atoms show slightly less dispersion and sharper peaks around −4 eV.

The valence p states of the Tr atoms are mostly filled at E_F, whereas occupancies of the Au 6p are significantly less (we compared the DOS ratio 6p/6s vs *E*). The Tr s states fall within and below the region of the dominant Au band, whereas the Tr *n*p are mainly involved in Tr−Tr bonding closer to E_F (Supporting Information, Figure S4). Involvement of the cations in the overall bonding is evident; their contributions to the valence band are almost equally distributed among their valence s, p, and d orbitals, the last particularly in the regions of the Au 5d bands. In other words, the active metals are not mere electron donors, which is of particular note when their environments in the structures are considered (below).

A look at the COHP curves accumulated over all bonds per unit cell (Figure 7b) shows that the stabilization of the structures is mainly provided by the aggregation of Au atoms. However, this dominance arises largely because of the sheer number of Au−Au interactions, inasmuch as the Au−Au/Tr−Au/Tr−Tr bonds per cell vary as 7:2:1 and 4:2:1 for **I/II** and **III**. In these terms, the alternative plots of average −ICOHP values for each bond type in Figure 7c give clearer pictures of the magnitudes of the individual pairwise contributions. These are more explicitly compared in Table 4 for each bond type according to distance, the integrated −ICOHP value, and the multiplicity of each per cell. The values for the different Au−Au interactions follow the distances fairly well, except for the somewhat greater magnitude for Au2−Au2, the six-bonded atoms, suggesting that the short and long pairings in both compounds are more intrinsic than the result of just matrix effects. For the larger Tr−Tr separations, the In−In −ICOHP value is somewhat greater than that for its congener Tl−Tl at about the same distance. The −ICOHP values for the different Au−Au interactions in all three compounds are roughly in the same range with slightly higher values for Au2−Au2, and these compare well with those from a model calculation for Au−Au interactions in hypothetical "NaAu" versus NaIn.[40]

A seemingly remarkable feature is that the proportions of short heteroatomic Au−Tr bonds for these compositions are not more numerous, inasmuch as they exhibit the highest −ICOHP values of all, as before;[32,37]

(40) For comparison, LMTO calculations were done on hypothetical "NaAu" with the lattice parameters and atomic positions of NaIn.[31a]

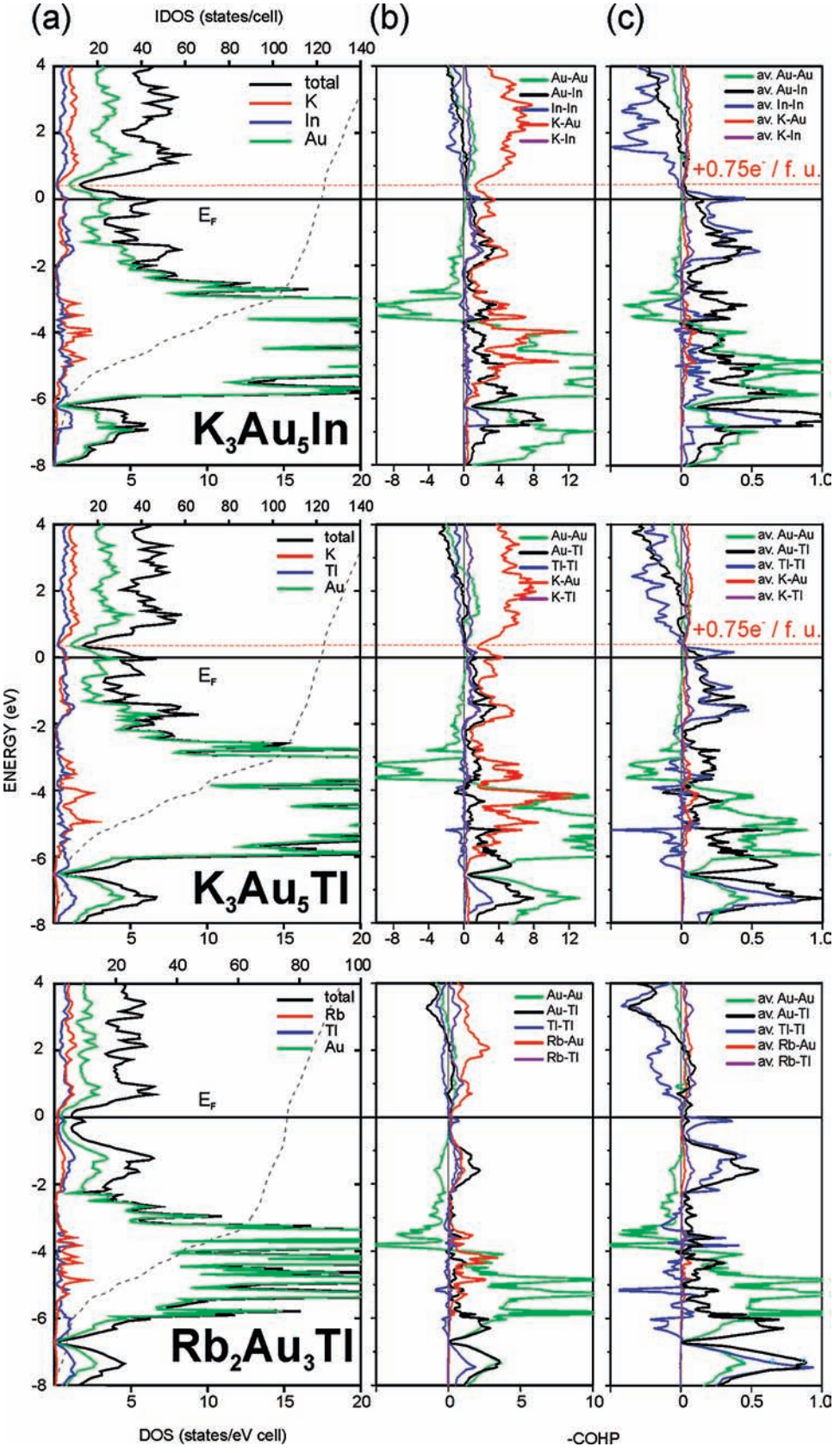

Figure 7. (a) DOS (total and partial), (b) total −COHP/cell, and (c) average −COHP data obtained from LMTO calculations for (top) K_3Au_5In, (middle) K_3Au_5Tl, and (bottom) Rb_2Au_3Tl. The Fermi level is set to 0 eV (black line), and the pseudogap energies are indicated by dotted red lines.

rather, 50% of the bonds to Tr are segregated into more weakly bound homoatomic Tr chains. However, both the sheer numbers of A−Au interactions in **I/II**, although significantly weaker per bond, and the fact that mainly

Table 4. Bond Distances [Å] and −ICOHP Values (eV/bond mol) for Different Interactions up to 4.0 Å in K_3Au_5In (**I**), K_3Au_5Tl (**II**), and Rb_2Au_3Tl (**III**)[a]

	I			II		III		
atom pair	distance	−ICOHP	*n*	distance	−ICOHP	distance	−ICOHP	*n*
Au1−Au2	2.780(1)	1.42	8	2.767(1)	1.43	2.790(1)	1.37	4
Au1−Au3	2.868(1)	1.10	4	2.856(1)	1.17			
Au1−Au1						2.825(2)	1.14	2
Au2−Au2	2.781(1)	1.53	8	2.798(1)	1.42	2.830(1)	1.41	2
Au2−Au3	2.848(1)	1.32	8	2.808(1)	1.43			
Au1−Tr	2.668(1)	2.32	8	2.715(1)	2.04	2.730(2)	1.96	4
Tr−Tr	3.136(2)	1.12	4	3.154(2)	0.83	3.134(1)	0.96	2
A−Au	3.295−3.624	0.17	104	3.309−3.702	0.21	3.474−3.848	0.17	36
A−Tr	3.651−3.891	0.17	20	3.669−3.849	0.24	3.827−3.994	0.12	10

[a] *n* is the number of interactions per unit cell. Au−Au/Au−Tr/Tr−Tr bond-type ratios are 7:2:1 and 4:2:1 per unit cell for **I**/**II** and **III**, respectively.

Table 5. Individual and Cumulative −ICOHP Components (eV/bond mol) in K_3Au_5Tr[a]

	Au−Au	Au−Tr	Tr−Tr	K−Au	K−Tr
per bond	1.38	2.18	0.98	0.19	0.20
number per unit cell	28	8	4	104	20
unit cell total	38.6	17.4	3.9	19.8	4.0
%	46	21	5	24	5

[a] Average for **I**/**II**, Table 4.

bonding states are occupied contribute to further stabilization of the structures. The overall effects are analyzed in Table 5 in terms of the individual −ICOHP values for each type of interaction for both the individual bond types and for the whole unit cell, using multiplicities and the average of −ICOHP data for **I** and **II** from Table 4, since the two show only small differences. Although −ICOHP data for bonds between different atom types are not comparable quantitatively, the general trends are clearly highlighted in the last two rows as Σ(−ICOHP) and percentile values. The dominance of Au−Au bond populations plus of the order of 24% of the total originating from the numerous K−Au contributions do give support for the idea that the A−Au bonding has a considerable influence on structure choice with its unusual segregation of Au−Au relative to Au−Tr bonding. Of course, we have no idea what the other unseen compositional and structural alternatives might be.

Thoughts on Electron Counting. Electron counting for the title phases is hampered by the clustering, the unusual properties and high coordination of Au, and the participation of the cations in the bonding. However, putting aside earlier ideas about cationic Au(I)−Au(I) interactions via closed-shell 5d−5d effects and d/s/p orbital mixing,[41] one can obtain an approximate electron count on the basis of the Zintl concept, as follows: Electron transfer from the alkali metal atoms to the [Au−Tr] networks takes place in all cases—the lower part of the "anion band" still reflects a sense of that disposition. Starting with Rb_2Au_3Tl, a Zintl formalism would be $2\{Rb^+\}\{Au_3Tl\}^{2-}$. Per formula unit, there are 2 × Au1, 2/2 × Au2, 2/2 × Tl, and 2 × Rb. Assuming the presence of a $\{4b-Tl\}^-$ and no $5d^{10}$ contributions from the start, one electron each from Rb and the three from the Au atoms are available for cluster bonding, a total of four electrons. Two might go to finish 2c−2e bonds to In (recall the large −ICOHP for Au−Tr) and two into a 4c−2e multicenter bond[49] within each Au_4 unit, leaving compound **III** charge-balanced, consistent with the pseudogap at E_F.

For K_3Au_5Tr, the same treatment results in $3\{K^+\}\{Au_5Tr\}^{3-}$. There are 2 × Au1, 2 × Au2, 1× Au3, 1× Tr, and 3 × K per formula unit, giving 11 valence electrons. Four are assigned to the Tr atom, as before, leaving five available for bonding among Au atoms and two to finish the *exo*-bonds to Tr. The central repeating pair of tetrahedra in the chain (vertical in Figure 2a) are composed of $(Au1)_2(Au2)_{4/2}(Au3)Tl_{2/2}$. If four electrons are required to bond these two vertex-sharing tetrahedra (or 12 edges), one electron is left unassigned.

Gold as a simple anion has been discussed previously for alkali-metal aurides, such as the semiconductors CsAu and RbAu (CsCl type).[43] In ternary phosphine cluster compounds, a $Au(PPh_3)$ fragment is considered as isolobal with CH_3 or H, meaning that its bonding characteristics are mainly determined by a singly occupied sp_z hybrid and empty higher-lying $p_{x,z}$ orbitals.[44] Cationic gold clusters in molecular compounds, for example, $\{Au_4\}^{2+}$, have been categorized in terms of their isolobal relationship with $\{H_4\}^{2+}$.[45] The Au−Au distances in $Au_4(PPh_3)_4I_2$[46] (2.65−2.83 Å) are comparable to those in the present cases, but slightly larger with respect to Au single-bond radii,[47] as perhaps expected for either the electron-deficient multicenter bonding or "core repulsions". However, single-bond distances in the supposed "$[Au-Au]^{\sim 4-}$" Zintl anions (2.85 Å) are also in the same range.[48] Recent investigations indicate that 4c−2e bonding within vertex-sharing Au_4 tetrahedra should also occur for neutral Au species.[42a] Nevertheless, the unbalanced scenario for **I**/**II** and other related phases suggests that these gold phases are positioned in an electronic region in which applications of simple electron counting schemes and simple structural motifs are more

(41) Pyykkö, P. *Chem. Soc. Rev.* **2008**, *37*, 1967.

(42) (a) Zubarev, D. Y.; Boldyrev, A. I. *J. Phys. Chem. A* **2009**, *113*, 866. (b) King, R. B. *Inorg. Chim. Acta* **1998**, *277*, 202.

(43) Jansen, M. *Chem. Soc. Rev.* **2008**, *37*, 1826 and references therein.

(44) Mingos, D. M. P. *Philos. Trans. R. Soc. London* **1982**, *A308*, 75.

(45) Burdett, J. K.; Eisenstein, O.; Schweizer, W. B. *Inorg. Chem.* **1994**, *33*, 3261.

(46) Demartin, F.; Manassero, M.; Naldini, L.; Ruggeri, R.; Sansoni, M. J. *Chem. Commun.* **1981**, 222.

(47) (a) Atsumi, M.; Pyykkö, P. *Chem.—Eur. J.* **2009**, *15*, 186. (b) Pauling, L. *J. Am. Chem. Soc.* **1947**, *69*, 542.

(48) Köhler, J.; Whangbo, M.-H. *Chem. Mater.* **2008**, *20*, 2751.

Table 6. Examples of (top) Ternary Structures in Au-Rich Triel and Tetrel Systems with [Au/(Tr,Tt)] ≥ 3, (middle) Binary Phases Containing Au_4 Tetrahedra, and (bottom) Some Other Novel Examples with 1 ≤ [Au/(Tr,Tt)] ≤ 2

e/a†[a]	compound	structural motifs	ref	e/a_{MX}
1.67	K_4Au_8Ga	filling variant of $NaAu_2$	34	1.15
1.83	K_3Au_5(In, Tl)	sheets of Au_4 linked by zigzag Tr chains	this work	1.22
1.96	$K_{12}Au_{21}Sn_4$	puckered sheets of Au_4	36	1.32
2.00	K_3Au_5Pb	isotypic with K_3Au_5(In, Tl)	15	1.33
2.00	Rb_2Au_3Tl	chains of Au_4 linked by zigzag Tl chains	this work	1.33
2.11	$A_4Au_7(Ge, Sn)_2$, (A = K, Rb, Cs)	Au_4 pairs bridged by Tt_2	16−18	1.46
1.80[b]	$CaAu_4Bi$	Au_4(Bi) nets; substituted $CaAu_5$	51	1.50[b]
2.01	$Ca_3Au_{12.2}In_{6.3}$	1/1AC; four endohedral, mixed In/Au shells	39	1.73
2.08	$Ca_4Au_{10}In_3$	wavy Au layers linked by In	32	1.59
1.40	$CaAu_5$	substituted $NaAu_2$; Ca@Au_{12} and Au@Au_{12} units[c]	52	1.17
1.40	(Sr,Ba)Au_5	hexagonal $CaCu_5$ type[d]	53	1.17
1.50	$NaAu_2$	cubic $MgCu_2$ type, all-vertex-sharing Au_4	14	1.00
	KAu_2	hexagonal $MgZn_2$ type[e]	54	1.00
1.20	(K,Rb)Au_5	hexagonal $CaCu_5$ type[c]	55	1.00
1.43	Rb_3Au_7	zigzag chains of Au_4 interconnected by square planar Au	35	1.00
2.00[b]	$PbAu_2$	$MgCu_2$ type (*Hunchunite*)	56	1.33[b]
2.50[b]	$BiAu_2$	$MgCu_2$ type (*Maldonite*)	57	1.67[b]
1.83	AAu_4In_2 (A = K, Rb)	Au/In tunnels centered by K	11	1.57
1.98	$K_{1.76}Au_6In_4$	Au/In tunnels centered by K	12	1.68
2.18	$K_{0.73}Au_2In_2$	Au/In tunnels centered by K	12	1.85
2.67	KAu_3Sn_3	$SrAu_3In_3$ type;[f] K@$Au_{10}Sn_{10}$ polyhedra	37	2.29
2.63	$RbAu_4Sn_4$	Rb@$Au_{12}Sn_{12}$ condensed polyhedra	36	2.33

[a] Counted as Zintl phases, electrons per network atom. The Au $5d^{10}$ shells are omitted from the electron counts. [b] LMTO calculations on these compounds reveal that the 6s orbitals for Bi and Pb are narrow and lie below the Au 5d band; they are therefore treated as core and not included in the e/a counts. [c] Inverse $AuBe_5$ type: Misch, L. *Metallwiss.* **1935**, *14*, 897. [d] All-vertex-sharing trigonal bipyramids with formally 6b-apex and 8b-waist a toms; some *face-sharing* tetrahedra. [e] Trigonal bipyramids that share 6b-apex atoms and are connected through *exo*−bonds at 6b-waist atoms; some *face-sharing* tetrahedra. [f] Muts, I. R.; Schappacher, F. M.; Hermes, W.; Zaremba, V. I.; Pöttgen, R. *J. Solid State Chem.* **2007**, *180*, 2202.

and more impaired by other factors, such as optimal packing, both nominal closed-shell d^{10} and cation involvement in the bonding, and relativistic effects.

A General Region of Novel Gold Clustering in Intermetallic Systems. Unique clustering of gold has now been uncovered for an appreciable number of electron-poorer gold compounds and structures in the present and related A−Au−In,Tl,Sn,Pb systems.[11,12,15−18,36,37] Electron counting rules suitable for Zintl phases classically assign valence electrons from the active (alkali, alkaline-earth, etc.) metals to the lower-lying orbital states of the polyanions in order to account for nominal closed-shell electronic structures (octet configurations) among the more electronegative p elements.[1,2] In these more familiar situations, $e/a^{\dagger}$ values (valence electrons per network atom) pertain to the total electron count distributed over just the number of atoms in the anions, and bona fide members have $e/a^{\dagger} > 4.0$. Some alkali-metal compounds containing isolated Ga, In, or Tl polyanions without gold still appear to achieve or approach more modern classes of closed-shell states, as enumerated by Wade's rules for the "electron-deficient" bonding in polyborane deltahedra, and so forth. In practice, however, well-bound electrons and semiconduction in the polytriel salts seldom pertain.[1,2]

In contrast, the generally electron-poorer polar intermetallic compounds (as distinguished from alloys) commonly exhibit valence electron distributions that extend over more-or-less all metal atom types, and so e/a_{MX} values calculated over all atoms are usually used to classify and discuss these. Quasicrystals and their approximants are good examples of the latter, and these often incorporate somewhat less electropositive elements, which include Li, Mg, Ca, or Sc, together with p elements from the tetrels and those to the left, including gold. Their e/a_{MX} values range from 1.7 to 2.2, broadly speaking.[32,39,49] Related special electronic states and pseudogaps near the Fermi energy have long been associated with the special class of less polar Hume−Rothery "electron compounds" with $\sim 1.3 < e/a_{MX} < 1.7$ that form between late transition and early p metals.[50]

Strict separation of the present polar intermetallic phases into either of these two categories does not seem very suitable, as these are so far limited to the more electropositive alkali metals, gold, and members of the Tr or Tt families, although a relationship with the QC approximants and their neighbors may be closer. This new category appears structurally unique for both the present condensed gold tetrahedra and the recently reported A−Au−Tr tunnel and A−Au−Sn network structures. These and other scattered examples together with

(49) Lin, Q.; Corbett, J. D. *Struct. Bonding (Berlin)* **2009**, *133*, 1.
(50) (a) Miller, G. J.; Lee, C.-S.; Choe, W. In *Inorganic Chemistry Highlights*; Meyer, G., Naumann, D., Wesemann, L., Eds.; Wiley-VCH Verlag-Gmbh: Weinheim, Germany, 2002; Chapter 2. (b) Mizutani, U.; Takeuchi, T.; Fournée, V.; Sato, H.; Banno, E.; Onogi, T. *Scripta Mater.* **2002**, *44*, 1181.
(51) Lin, Q.; Corbett, J. D. To be submitted for publication.
(52) Raub, C. J.; Hamilton, D. C. *J. Less-Common Met.* **1964**, *6*, 486.
(53) Palenzona, A. *Atti Accad. Nazl. Lincei Cl. Sci. Fis. Mat. Nat. Rend.* **1967**, *42*, 504.
(54) Range, K. J.; Rau, F.; Klement, U. *Acta Crystallogr., Sect. C* **1988**, *44*, 1485.
(55) Raub, C. J.; Compton, V. B. *Z. Anorg. Allg. Chem.* **1964**, *332*, 5.
(56) Perlitz, H. *Strukturber.* **1934**, *3*, 612.
(57) Jurriaanse, T. *Z. Kristallogr.* **1935**, *90*, 322.

some relevant binary examples, primarily derived from $MgCu_2$, are listed in three categories in Table 6 along with their e/a counts on both scales.

The ternary phases in the top portion are positioned in an intermediate region with particularly low e/a values when expressed either over all atoms, more appropriate to Hume−Rothery or Laves intermetallic systems (e/a_{MX} 1.1∼1.7), or just over the "polyanionic" networks as particularly electron-poor "*Zintl* phases", as $e/a^{\dagger} = 1.7-2.1$. The former is probably more appropriate. A strong competition between electronic and size factors is perhaps implied. In either case, these e/a measures include a single valence electron for gold (in order to avoid numerical discontinuities), although it is very clear that Au 5d orbitals and electrons are involved in bonding. A further differentiation of this group is reasonable, as the most pronounced features are the relative number of cations and e/a. On average, the coupling of larger cation and gold proportions (smaller e/a values) affords more open assemblies with evidently significant cation involvement in the bonding, as in the structures of **I**/**II** and **III**. At one extreme, the binary Laves phases and their derivatives in the middle group of the table have a smaller fraction of cations, or none at all, and exhibit the upper limits of condensed gold networks, largely deriving from cubic $MgCu_2$ (Figure S5, Supporting Information) or hexagonal $MgZn_2$ parents. (The unusual substitution of Bi or Pb into some gold networks can be understood a bit better when it is realized that their $6s^2$ levels are more corelike.[51]) Finally, the somewhat arbitrary group in the bottom third of Table 6 may at this time contain only fragments of a new family of gold compounds with lower alkali-metal and higher triel/tetrel proportions in cation-centered tunnels or polyhedra. As a whole, this last group of ternary and still relatively electron-poor systems will very likely expand and diverge with time and more exploration, as the electropositive element and gold are the only common theme at present. Unusual platinum analogues have not yet been uncovered, and distinctive ternary mercury examples have not been seen so far (except perhaps for $BaHg_2Tl_2$[58]), whereas silver has played only more normal roles in a few investigations.[3]

The present results beautifully illustrate the opportunities that exist during a search for new compounds with unanticipated structures in unexplored phase spaces, especially because so little is known about even the multitude of possible ternary systems.[59] The utter surprise realized on discovery of *five* different structures built of condensed Au−In tunnels centered by K (or other alkali metal cations)[11,12] naturally led us to look for the Tl analogues, starting with comparable AAu_4Tl_2 compositions. Such good intentions were instead rewarded by the appearance of two distinctly gold-richer networks that are built of chains or sheets of condensed gold tetrahedra interlinked by zigzag thallium chains. The indium analogue that followed then became the *sixth* ternary network phase in the K−Au−In system!

Acknowledgment. This research was supported by the Office of the Basic Energy Sciences, Materials Sciences Division, U.S. Department of Energy (DOE). Ames Laboratory is operated for DOE by Iowa State University under contract No. DE-AC02-07CH11358.

Supporting Information Available: Single crystal refinement data for the title compounds in CIF format, Figures of cation environments, fat-band diagrams, DOS plots of Au 5d-band splittings and of separate orbital contributions for all atoms, and a figure of the $NaAu_2$ structure. These materials are available free of charge via the Internet at http://pubs.acs.org.

(58) Dai, J.-C.; Gupta, S.; Gourdon, O.; Kim, H.-J.; Corbett, J. D. *J. Am. Chem. Soc.* **2009**, *131*, in press.

(59) DiSalvo, F. J. *Pure Appl. Chem.* **2000**, *72*, 1799.